

TIME-DOMAIN INTEGRAL EQUATION SOLVER FOR RADIATION FROM DIPOLE ANTENNA LOADED WITH GENERAL BI-ISOTROPIC OBJECTS

H. Zhu^{1,*}, Z.-H. Wu², X.-Y. Zhang¹, and B.-J. Hu¹

¹The Guangdong Provincial Key Laboratory of Short-Range Wireless Detection and Communication, School of Electronic and Information Engineering, South China University of Technology, Guangzhou 510640, China

²Argus Technologies (China) Ltd., Guangzhou 510730, China

Abstract—Electromagnetic radiation by dipole antenna loaded with general bi-isotropic objects is investigated using time-domain integral equations. By introducing pairs of equivalent electric and magnetic sources, electromagnetic fields inside a homogeneous bi-isotropic region can be represented by these sources over its boundary. A series of coupled surface integral equations are obtained after imposing boundary conditions. These equations are solved numerically by the Galerkin's method that involves separate spatial and temporal testing procedures. The scaled Laguerre functions are used as the temporal basis and testing functions. The use of the Laguerre functions completely removes the time variable from computation, and the results are stable even at late times. Numerical results are presented and compared with analytical results, and similarities and differences are observed.

1. INTRODUCTION

In the last two decades or so, Bi-isotropic (BI) medium has emerged as one of the most challenging topics in electromagnetic research in terms of theoretical problems and potential applications [1]. Among all these new materials, Chiral and Tellegen materials represent two subclasses of BI medium [2, 3]. Chiral medium is optically active, and it means that the polarization plane of an electromagnetic (EM) wave is rotated when propagating through it. Investigations show that Chiral

Received 19 August 2011, Accepted 5 October 2011, Scheduled 2 November 2011

* Corresponding author: Hui Zhu (zhuhui@lifudv.com).

medium possesses the property of reciprocity, while Tellegen medium is nonreciprocal. Many efforts have been made in the fabrication of these BI materials [4–6] because of their great potential in the millimeter-wave and microwave applications such as antenna radomes [7], chiro-microstrip antennas [8], modes convertors [9], and polarization rotators [10]. Such material brings about new challenges to the EM theory since its constitutive relationships enforce an additional coupling between electric and magnetic fields. Hence, many works have been contributed in an effort to develop an efficient numerical technique to predict accurately the field's interaction associated with such materials [11–16].

This paper is focused on the electromagnetic radiation from a dipole antenna interacting with a BI object. The exact formulation has been proposed by Engheta and Kowarz [16] for radiation emitted by EM sources placed both inside and outside Chiral sphere. The eigenfunction expansion in spherical coordinates was used in this solution, and the dyadic Green's functions were expressed in terms of spherical vector functions. However, this formula is restricted to Chiral spheres, therefore it is of great interest to obtain a general solution for BI objects with arbitrary shape. In addition, the results on the radiation of the antenna located in the Chiral sphere were only given, and the case of the antenna outside the BI objects, which is of our interest, needs to be analyzed as well.

The time-domain integral equation (TDIE) solver is commonly used for analyzing complex EM scattering and radiation phenomenon [17–23]. Although the finite-different time-domain (FDTD) method has been the dominant tool for time-domain simulations [17], the TDIE approach is preferable in some applications especially for analysis of transient scattering by large-size bodies. The reason is that the TDIE method solves fewer unknowns using surfaces discretization and requires no artificial absorbing boundary condition (ABC). The most popular method to solve a TDIE is the marching-on in time (MOT) scheme [18–20]. However, many researchers have pointed that the MOT method may suffer from late-time instabilities in the form of high frequency oscillation. Recently, the marching-on in degree (MOD) method [21–23] using a set of scaled Laguerre polynomials as the temporal expansion and testing functions is proposed for the TDIE, and stable results can be obtained even for late time. Wu used this method to deal with the scattering problems by BI media in [24], and this work presents the extension of the MOD-based TDIE method for dipole antenna near the three-dimensional homogeneous BI object with arbitrarily shape.

In the paper, pairs of new sources and two integro-differential

operators are defined and introduced to formulate the far scattered fields by homogeneous dielectric objects in time domain. Then the method is extended for constructing scattered fields inside and outside the BI medium, and far radiated fields by the dipole as well. The electromagnetic fields inside a homogeneous bi-isotropic region can be represented by the equivalent sources over its boundary after applying fields splitting method [1]. After enforcing boundary conditions both on the surface of the BI object and the dipole, a series of coupled integral equations are established and solved numerically by the method of moment (MoM) [25], involving spatial and temporal testing procedures separately. The Rao-Wilton-Glisson (RWG) [26] functions are used as the spatial expansion and testing functions, and the weighted Laguerre functions are used as the temporal expansion and testing functions. The spatial testing is performed at the first step, and then the temporal testing is employed. The use of the Laguerre functions completely removes the time variable from the whole computation, and the matrix equation is solved recursively using a MOD procedure. The transient currents, the current distribution along the dipole and far radiation fields are presented and compared to validate the proposed TDIE method.

2. THEORY AND EQUATIONS

2.1. Equivalent Sources for Homogeneous Dielectric Bodies

Consider a homogeneous dielectric body with a permittivity of ε_2 and a permeability of μ_2 in an infinite homogeneous medium with a permittivity of ε_1 and a permeability of μ_1 . Pairs of new sources $\mathbf{e}(\mathbf{r}, t)$ and $\mathbf{h}(\mathbf{r}, t)$ [23] on the surface S of the dielectric body are defined by

$$\mathbf{J}(\mathbf{r}, t) = \frac{\partial}{\partial t} \mathbf{e}(\mathbf{r}, t) \quad (1)$$

$$\mathbf{M}(\mathbf{r}, t) = \frac{\partial}{\partial t} \mathbf{h}(\mathbf{r}, t) \quad (2)$$

where $\mathbf{J}(\mathbf{r}, t)$ and $\mathbf{M}(\mathbf{r}, t)$ are the equivalent electric and magnetic surface current.

The electric and magnetic fields \mathbf{E}^s and \mathbf{H}^s produced by electric and magnetic surface currents \mathbf{J} and \mathbf{M} , radiating into an unbounded space characterized by ε_1 and μ_1 are given by

$$\mathbf{E}^s = -\frac{\partial \mathbf{A}(\mathbf{r}, t)}{\partial t} - \nabla \Phi(\mathbf{r}, t) - \frac{1}{\varepsilon_1} \nabla \times \mathbf{F}(\mathbf{r}, t) \quad (3)$$

$$\mathbf{H}^s = -\frac{\partial \mathbf{F}(\mathbf{r}, t)}{\partial t} - \nabla \Psi(\mathbf{r}, t) + \frac{1}{\mu_1} \nabla \times \mathbf{A}(\mathbf{r}, t) \quad (4)$$

where \mathbf{A} and \mathbf{F} are the magnetic and electric vector potentials, respectively, and Φ and Ψ are the electric and magnetic scalar potentials given by

$$\mathbf{A}(\mathbf{r}, t) = \frac{\mu_1}{4\pi} \int_s \frac{\mathbf{J}(\mathbf{r}', \tau)}{R} dS' \quad (5)$$

$$\mathbf{F}(\mathbf{r}, t) = \frac{\varepsilon_1}{4\pi} \int_s \frac{\mathbf{M}(\mathbf{r}', \tau)}{R} dS' \quad (6)$$

$$\Phi(\mathbf{r}, t) = \frac{1}{4\pi\varepsilon_1} \int_s \frac{q_e(\mathbf{r}', \tau)}{R} dS' \quad (7)$$

$$\Psi(\mathbf{r}, t) = \frac{1}{4\pi\mu_1} \int_s \frac{q_m(\mathbf{r}', \tau)}{R} dS' \quad (8)$$

where $R = |\mathbf{r} - \mathbf{r}'|$ represents the distance between the observation point \mathbf{r} and the source point \mathbf{r}' , $\tau = t - R/c_1$ is the retarded time, $c_1 = 1/\sqrt{\varepsilon_1\mu_1}$ is the velocity of the propagation of EM wave in space. The electric surface charge density q_e and magnetic surface charge density q_m are related to the electric current density \mathbf{J} and magnetic current density \mathbf{M} , respectively, by the equation of continuity

$$\nabla \cdot \mathbf{J}(\mathbf{r}, t) = -\frac{\partial}{\partial t} q_e(\mathbf{r}, t) \quad (9)$$

$$\nabla \cdot \mathbf{M}(\mathbf{r}, t) = -\frac{\partial}{\partial t} q_m(\mathbf{r}, t) \quad (10)$$

A pair of new sources $\mathbf{e}(\mathbf{r}, t)$ and $\mathbf{h}(\mathbf{r}, t)$ are defined in (1) and (2), so the charge density will be

$$q_e(\mathbf{r}, t) = -\nabla \cdot \mathbf{e}(\mathbf{r}, t) \quad (11)$$

$$q_m(\mathbf{r}, t) = -\nabla \cdot \mathbf{h}(\mathbf{r}, t) \quad (12)$$

Equations (5)–(8) will be changed as

$$\mathbf{A}(\mathbf{r}, t) = \frac{\mu_1}{4\pi} \int_s \frac{1}{R} \frac{\partial}{\partial t} \mathbf{e}(\mathbf{r}', \tau) dS' \quad (13)$$

$$\mathbf{F}(\mathbf{r}, t) = \frac{\varepsilon_1}{4\pi} \int_s \frac{1}{R} \frac{\partial}{\partial t} \mathbf{h}(\mathbf{r}', \tau) dS' \quad (14)$$

$$\Phi(\mathbf{r}, t) = -\frac{1}{4\pi\varepsilon_1} \int_s \frac{1}{R} \nabla \cdot \mathbf{e}(\mathbf{r}', \tau) dS' \quad (15)$$

$$\Psi(\mathbf{r}, t) = -\frac{1}{4\pi\mu_1} \int_s \frac{1}{R} \nabla \cdot \mathbf{h}(\mathbf{r}', \tau) dS' \quad (16)$$

Substitute Equations (13)–(16) to (3) and (4), respectively,

$$\begin{aligned} \mathbf{E}^s = & -\mu_1 \int_S \frac{1}{4\pi R} \frac{\partial^2 \mathbf{e}(\mathbf{r}, \tau)}{\partial t^2} dS' + \frac{\nabla}{\varepsilon_1} \int_S \frac{\nabla \cdot \mathbf{e}(\mathbf{r}, \tau)}{4\pi R} dS' \\ & - 0.5\hat{n} \times \frac{\partial \mathbf{h}(\mathbf{r}, t)}{\partial t} - \int_{S_0} \nabla \times \frac{1}{4\pi R} \frac{\partial \mathbf{h}(\mathbf{r}, \tau)}{\partial t} dS' \end{aligned} \quad (17)$$

$$\begin{aligned} \mathbf{H}^s = & -\varepsilon_1 \int_S \frac{1}{4\pi R} \frac{\partial^2 \mathbf{h}(\mathbf{r}, \tau)}{\partial t^2} dS' + \frac{\nabla}{\mu_1} \int_S \frac{\nabla \cdot \mathbf{h}(\mathbf{r}, \tau)}{4\pi R} dS' \\ & + 0.5\hat{n} \times \frac{\partial \mathbf{e}(\mathbf{r}, t)}{\partial t} + \int_{S_0} \nabla \times \frac{1}{4\pi R} \frac{\partial \mathbf{e}(\mathbf{r}, \tau)}{\partial t} dS' \end{aligned} \quad (18)$$

where S_0 denotes the surface with the singularity at $\mathbf{r} = \mathbf{r}'$ removed from the surface S . We define two integro-differential operators L and K as follows,

$$L(\mathbf{X}) = \mu_1 \int_S \frac{\partial^2 \mathbf{X}(\mathbf{r}', \tau)}{\partial t^2} \frac{1}{4\pi R} dS' - \frac{\nabla}{\varepsilon_1} \int_S \frac{\nabla \cdot \mathbf{X}(\mathbf{r}', \tau)}{4\pi R} dS' \quad (19)$$

$$K(\mathbf{X}) = \frac{1}{2} \hat{n} \times \frac{\partial}{\partial t} \mathbf{X}(\mathbf{r}, t) + \int_{S_0} \nabla \times \left[\frac{\partial \mathbf{X}(\mathbf{r}', \tau)}{\partial t} \frac{1}{4\pi R} \right] dS' \quad (20)$$

Then, the total scattered electric and magnetic fields will be written as

$$E^s = -L(\mathbf{e}) - K(\mathbf{h}). \quad (21)$$

$$H^s = K(\mathbf{e}) - L(\mathbf{h})/\eta_1^2. \quad (22)$$

It is noted that here we introduce a pair of new sources $\mathbf{e}(\mathbf{r}, t)$ and $\mathbf{h}(\mathbf{r}, t)$ instead of using conventional equivalent electrical current $\mathbf{J}(\mathbf{r}, t)$ and magnetic current $\mathbf{M}(\mathbf{r}, t)$ to construct the far-scattered fields. Such that, a time-integral term will disappear, and we can easily handle the time derivative of the electric and magnetic vector potentials.

2.2. Integral Equations for BI medium Loaded Dipole Antenna

Consider a homogeneous BI body with a permittivity of ε_2 and a permeability of μ_2 in an infinite homogeneous medium with a permittivity of ε_1 and a permeability of μ_1 . Here, a very narrow perfectly electric conducting (PEC) strip is placed near the BI sphere as the loaded dipole, as shown in Figure 1. The length of the dipole is

L , the radius of the sphere is r , and the distance between the center of the dipole and the sphere's center is denoted as d . For the sake of simplicity, the dipole is put along the z -axis and centered at the origin, and the center of the BI sphere is located at the point $(0, d, 0)$.

The constitutive relationships between the flux densities and the field intensities can be expressed as

$$\mathbf{D} = \varepsilon_2 \mathbf{E} + (\chi_r - j\kappa_r) \sqrt{\varepsilon_2 \mu_2} \mathbf{H} \quad (23)$$

$$\mathbf{B} = (\chi_r + j\kappa_r) \sqrt{\varepsilon_2 \mu_2} \mathbf{E} + \mu_2 \mathbf{H} \quad (24)$$

where χ_r and κ_r are Tellegen and Pasteur parameters [1], and ε_2 and μ_2 are the permittivity and permeability of the BI Media, respectively. For a lossy material, these parameters are complex. It is noticed that the above relations reduce to a conventional isotropic medium when both χ_r and κ_r are equal to zero. A bi-isotropic medium with $\chi_r = 0$ and $\kappa_r \neq 0$ is named the Pasteur medium or Chiral medium, and it is named Tellegen medium conversely.

These relations are frequency-domain expressions, which implicitly assume time-harmonic excitation in the $e^{j\omega t}$ convention. The time-domain expressions of the constitutive relations are given as follows [27],

$$\mathbf{D} = \varepsilon_2 \mathbf{E} + \gamma_{CT} \mathbf{H} - \chi_{CT} \frac{\partial \mathbf{H}}{\partial t} \quad (25)$$

$$\mathbf{B} = \mu_2 \mathbf{H} + \gamma_{CT} \mathbf{E} + \chi_{CT} \frac{\partial \mathbf{E}}{\partial t} \quad (26)$$

where

$$\gamma_{CT} = \chi_r \sqrt{\varepsilon_2 \mu_2} \quad (27)$$

$$\chi_{CT} = \kappa_r \sqrt{\varepsilon_2 \mu_2} / \omega \quad (28)$$

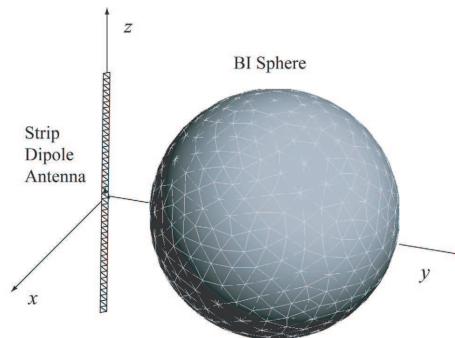


Figure 1. A strip dipole near a BI sphere.

The equivalent electric and magnetic sources on the dipole and the surface of the BI media are denoted as $\mathbf{e}_c(\mathbf{r}, t)$, $\mathbf{e}_b(\mathbf{r}, t)$ and $\mathbf{h}_b(\mathbf{r}, t)$, respectively, and surface currents are denoted as $\mathbf{J}_c(\mathbf{r}, t)$, $\mathbf{J}_b(\mathbf{r}, t)$, and $\mathbf{M}_b(\mathbf{r}, t)$, respectively, as shown in Figure 2. The currents $\mathbf{J}_c(\mathbf{r}, t)$, $\mathbf{J}_b(\mathbf{r}, t)$, and $\mathbf{M}_b(\mathbf{r}, t)$ can be expressed with these sources $\mathbf{e}_c(\mathbf{r}, t)$, $\mathbf{e}_b(\mathbf{r}, t)$ and $\mathbf{h}_b(\mathbf{r}, t)$ as

$$\mathbf{J}_c(\mathbf{r}, t) = \frac{\partial}{\partial t} \mathbf{e}_c(\mathbf{r}, t) \tag{29}$$

$$\mathbf{J}_b(\mathbf{r}, t) = \frac{\partial}{\partial t} \mathbf{e}_b(\mathbf{r}, t) \tag{30}$$

$$\mathbf{M}_b(\mathbf{r}, t) = \frac{\partial}{\partial t} \mathbf{h}_b(\mathbf{r}, t) \tag{31}$$

The far fields radiated from the dipole can be obtained using integro-differential operators in (19) and (20) as,

$$\mathbf{E}_c^s(\mathbf{e}_c) = -L(\mathbf{e}_c) \tag{32}$$

$$\mathbf{H}_c^s(\mathbf{e}_c) = K(\mathbf{e}_c) \tag{33}$$

where \mathbf{E}_c^s and \mathbf{H}_c^s are the radiated electric and magnetic fields.

Similarly, the scattered fields \mathbf{E}_e^s and \mathbf{H}_e^s outside the BI media produced by the sources \mathbf{e}_b and \mathbf{h}_b is written as

$$\mathbf{E}_e^s(\mathbf{e}_b, \mathbf{h}_b) = -L(\mathbf{e}_b) - K(\mathbf{h}_b)/\eta_1^2 \tag{34}$$

$$\mathbf{H}_e^s(\mathbf{e}_b, \mathbf{h}_b) = K(\mathbf{e}_b) - L(\mathbf{h}_b)/\eta_1^2 \tag{35}$$

To represent the fields in the BI region, a field splitting scheme [1] is applied. Both the electric and magnetic fields \mathbf{E}_b^s and \mathbf{H}_b^s in the homogeneous BI medium are divided into the right- and left-circularly polarized wavefields. The right-polarized fields are denoted by “+”

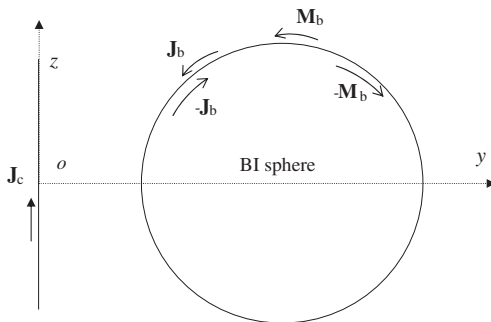


Figure 2. Currents on the dipole and the surface of the BI sphere.

subscript, while the left-polarized components are denoted by “-” subscript. Therefore, we can write

$$\mathbf{E}_b^s = \mathbf{E}_{b+}^s + \mathbf{E}_{b-}^s \quad (36)$$

$$\mathbf{H}_b^s = \mathbf{H}_{b+}^s + \mathbf{H}_{b-}^s \quad (37)$$

The wavefields $\mathbf{E}_{b+}^s(\mathbf{H}_{b+}^s)$ and $\mathbf{E}_{b-}^s(\mathbf{H}_{b-}^s)$ are independent and uncoupled in the homogeneous BI medium. They are related to respective medium characterized by ε_+ (ε_-), μ_+ (μ_-), and η_+ (η_-), which are defined by

$$\varepsilon_{\pm} = \varepsilon_2(\alpha \pm \kappa_r)v_{\pm} \quad (38)$$

$$\mu_{\pm} = \mu_2(\alpha \pm \kappa_r)v_{\mp} \quad (39)$$

$$\eta_{\pm} = \sqrt{\mu_2/\varepsilon_2}v_{\mp} = \eta_2v_{\mp} \quad (40)$$

where $v_{\pm} = \alpha \pm j\chi_r$ and $\alpha = \sqrt{1 - \chi_r^2}$. Since two wavefields are independently governed by Maxwell's equations, $\mathbf{E}_{b+}^s(\mathbf{H}_{b+}^s)$ and $\mathbf{E}_{b-}^s(\mathbf{H}_{b-}^s)$ can be expressed by

$$\mathbf{E}_{b\pm}^s = -L_{\pm}(\mathbf{e}_{b\pm}) - K_{\pm}(\mathbf{h}_{b\pm}) \quad (41)$$

$$\mathbf{H}_{b\pm}^s = K_{\pm}(\mathbf{e}_{b\pm}) - L_{\pm}(\mathbf{h}_{b\pm})/\eta_{\pm}^2 \quad (42)$$

where the integro - differential operators L_{\pm} and K_{\pm} are defined as

$$L_{\pm}(\mathbf{X}) = \mu_{\pm} \int_S \frac{\partial^2 \mathbf{X}(\mathbf{r}', \tau)}{\partial t^2} \frac{1}{4\pi R} dS' - \frac{\nabla}{\varepsilon_{\pm}} \int_S \frac{\nabla \cdot \mathbf{X}(\mathbf{r}', \tau)}{4\pi R} dS' \quad (43)$$

$$K_{\pm}(\mathbf{X}) = \int_{S_0} \nabla \times \left[\frac{\partial \mathbf{X}(\mathbf{r}', \tau)}{\partial t} \frac{1}{4\pi R} \right] dS' - \frac{1}{2} \hat{n} \times \frac{\partial}{\partial t} \mathbf{X}(\mathbf{r}, t) \quad (44)$$

As can be seen, the expressions of the scattered wavefields $\mathbf{E}_{b+}^s(\mathbf{H}_{b+}^s)$ and $\mathbf{E}_{b-}^s(\mathbf{H}_{b-}^s)$ in the media induced by $\mathbf{e}_{b+}(\mathbf{h}_{b+})$ and $\mathbf{e}_{b-}(\mathbf{h}_{b-})$ are similar to those of free space except that the material parameters are different. Here the relations of $(\mathbf{e}_b, \mathbf{h}_b)$ and $(\mathbf{e}_{b+}(\mathbf{h}_{b+}), \mathbf{e}_{b-}(\mathbf{h}_{b-}))$ can be obtained from Maxwell's equations [24],

$$-\mathbf{e}_{b\pm} = \frac{1}{2\alpha}(v_{\pm}\mathbf{e}_b \mp \frac{j}{\eta_2}\mathbf{h}_b). \quad (45)$$

$$-\mathbf{h}_{b\pm} = \frac{1}{2\alpha}(v_{\mp}\mathbf{h}_b \pm j\eta_2\mathbf{e}_b). \quad (46)$$

To determine the unknown sources \mathbf{e}_c , \mathbf{e}_b and \mathbf{h}_b , the boundary condition needs to be enforced on the surface of the strip dipole and the BI scatterer. On the surface of the dipole, the tangential components of the total electric fields must vanish, that is

$$-\mathbf{E}_c^s(\mathbf{e}_c)|_{\text{tan}} - \mathbf{E}_e^s(\mathbf{e}_b, \mathbf{h}_b)|_{\text{tan}} = \mathbf{E}^{\text{in}}(\mathbf{r}, t)|_{\text{tan}} \quad (47)$$

where subscript “tan” defines tangential components, \mathbf{E}^{in} is the excited electric field. By enforcing boundary condition on the interface between BI media and the outside space, we can obtain two coupled integral equations as follows

$$-\mathbf{E}_c^s(\mathbf{e}_c)|_{\text{tan}} - \mathbf{E}_e^s(\mathbf{e}_b, \mathbf{h}_b)|_{\text{tan}} + \sum_{\pm} \mathbf{E}_{b\pm}^s(\mathbf{e}_{b\pm}, \mathbf{h}_{b\pm})|_{\text{tan}} = 0 \quad (48)$$

$$-\mathbf{H}_c^s(\mathbf{e}_c)|_{\text{tan}} - \mathbf{H}_e^s(\mathbf{e}_b, \mathbf{h}_b)|_{\text{tan}} + \sum_{\pm} \mathbf{H}_{b\pm}^s(\mathbf{e}_{b\pm}, \mathbf{h}_{b\pm})|_{\text{tan}} = 0 \quad (49)$$

2.3. Basis Functions and Testing Scheme

MoM is adopted to solve the equation series (47)–(49). For the numerical implementation, the equivalent electric and magnetic currents $\mathbf{e}_c(\mathbf{r}, t)$, $\mathbf{e}_b(\mathbf{r}, t)$ and $\mathbf{h}_b(\mathbf{r}, t)$ are represented in terms of RWG functions [26]

$$\mathbf{e}_c(\mathbf{r}, t) = \sum_{n=1}^{N_c} \sum_{j=0}^{\infty} e_{cn,j} \varphi_j(st) \mathbf{f}_n(\mathbf{r}) \quad (50)$$

$$\mathbf{e}_b(\mathbf{r}, t) = \sum_{n=1}^{N_b} \sum_{j=0}^{\infty} e_{bn,j} \varphi_j(st) \mathbf{f}_n(\mathbf{r}) \quad (51)$$

$$\mathbf{h}_b(\mathbf{r}, t) = \sum_{n=1}^{N_b} \sum_{j=0}^{\infty} h_{bn,j} \varphi_j(st) \mathbf{f}_n(\mathbf{r}) \quad (52)$$

where N_c and N_b are the numbers of the inner edges on the dipole and the BI scatterer, respectively, $e_{cn,j}$, $e_{bn,j}$ and $h_{bn,j}$ are the unknown coefficients, and $\phi_j(st) = e^{-st/2} L_j(st)$ are the causal temporal basis functions. $L_j(st)$ is the Laguerre function [28] of order j with a scaling factor s , and $\mathbf{f}_n(\mathbf{r})$ represents the RWG function.

Substituting (50)–(52) to (19) and (20) respectively, we obtained

$$\begin{aligned} L(\mathbf{e}_c) = & \mu_0 s^2 \sum_{n=1}^{N_c} \sum_{j=0}^{\infty} \int_S \frac{1}{4\pi R} \left(0.25 e_{cn,j} + \sum_{k=0}^{j-1} (j-k) e_{cn,k} \right) \phi_j(s\tau) \mathbf{f}_n(\mathbf{r}) dS' \\ & - \frac{1}{\epsilon_0} \sum_{n=1}^{N_c} \sum_{j=0}^{\infty} e_{cn,j} \nabla \int_S [\nabla \cdot \mathbf{f}_n(\mathbf{r})] \frac{\phi_j(s\tau)}{4\pi R} dS' \end{aligned} \quad (53)$$

$$\begin{aligned}
K(\mathbf{e}_c) &= 0.5\hat{n}\times s \sum_{n=1}^{N_c} \sum_{j=0}^{\infty} \left(0.5e_{cn,j} + \sum_{k=0}^{j-1} e_{cn,k} \right) \phi_j(s\tau)\mathbf{f}_n(\mathbf{r}) \\
&\quad + \frac{s^2}{c_0} \sum_{n=1}^{N_c} \sum_{j=0}^{\infty} \int_{S_0} \left(0.25e_{cn,j} + \sum_{k=0}^{j-1} (j-k)e_{cn,k} \right) \phi_j(s\tau)\mathbf{f}_n(\mathbf{r}) \times \hat{R}/R dS' \\
&\quad + s \sum_{n=1}^{N_c} \sum_{j=0}^{\infty} \int_{S_0} \left(0.5e_{cn,j} + \sum_{k=0}^{j-1} e_{cn,k} \right) \phi_j(s\tau)\mathbf{f}_n(\mathbf{r}) \times \hat{R}/R^2 dS' \quad (54)
\end{aligned}$$

Since $L(\mathbf{e}_b)$ and $L(\mathbf{h}_b)$ are identical to $L(\mathbf{e}_c)$ in Equation (53), and $K(\mathbf{e}_b)$ and $K(\mathbf{h}_b)$ are identical to $K(\mathbf{e}_c)$ in (54), the formulations are omitted here.

In computing the spatial integrals in (53) and (54), the functions dependent on the following variable do not change appreciably within a given triangular patch so that

$$\tau_v = t - \frac{R}{c_v}, \quad \tau_{mn}^{pq}, v = t - \frac{R_{mn}^{pq}}{c_v}, \quad R_{mn}^{pq} = |\mathbf{r}_m^{cp} - \mathbf{r}_n^{cq}| \quad (55)$$

where p, q , and v can be either $+$ or $-$, and \mathbf{r}_m^{cp} and \mathbf{r}_n^{cq} are the position vectors of the center points in triangle pair T_m^\pm .

Through the Galerkin's method [25], we take a spatial and a temporal testing with $\mathbf{f}_m(\mathbf{r})$ ($m=1, 1, 2 \dots N_c$) and $\phi_i(st)$ ($i=0, 1, 2 \dots M$) separately to the Equation (47), where M is the maximum order of the Laguerre functions to be evaluated from the time-bandwidth product of the waveform. The equation below is obtained

$$\begin{aligned}
&\langle \phi_i(st), \langle \mathbf{f}_m(\mathbf{r}), L(\mathbf{e}_c) \rangle \rangle + \langle \phi_i(st), \langle \mathbf{f}_m(\mathbf{r}), L(\mathbf{e}_b) \rangle \rangle \\
&\quad + \langle \phi_i(st), \langle \mathbf{f}_m(\mathbf{r}), K(\mathbf{h}_b) \rangle \rangle = \langle \phi_i(st), \langle \mathbf{f}_m(\mathbf{r}), \mathbf{E}^{\text{in}} \rangle \rangle \quad (56)
\end{aligned}$$

First, we consider the testing of the integro-differential operator L with the electric source \mathbf{e}_c . With reference to [21], the testing formulation can be written as

$$\begin{aligned}
&\langle \phi_i(st), \langle \mathbf{f}_m(\mathbf{r}), L(\mathbf{e}_c(\mathbf{r}, t)) \rangle \rangle = \mu_0 s^2 \sum_{n=1}^{N_c} \sum_{p,q}^i \sum_{j=0}^i (0.25e_{cn,j} + \sum_{k=0}^{j-1} (j-k)e_{cn,k}) \\
&I_{ij}(s\tau_{mn}^{pq}) a_{mn,1}^{pq} + \frac{1}{\varepsilon_0} \sum_{n=1}^{N_c} \sum_{p,q}^i \sum_{j=0}^i e_{cn,j} I_{ij}(s\tau_{mn}^{pq}) b_{mn,1}^{pq} \quad (57)
\end{aligned}$$

where inner integral $\langle \mathbf{f}_m(\mathbf{r}), \rangle$ denotes a spatial testing which is defined by multiplying the function $\mathbf{f}_m(\mathbf{r})$ and integrating in the triangle pairs T_m^\pm on the PEC strip, and $\langle \phi_i(st), \rangle$ represents a temporal testing,

which is done by multiplying the function $\phi_i(st)$ and integrating from zero to infinity. The temporal testing can be simplified as

$$I_{ij}(s\tau_{mn}^{pq}) = \begin{cases} e^{-s\tau_{mn}^{pq}/2} [L_{i-j}(s\tau_{mn}^{pq}) - L_{i-j-1}(s\tau_{mn}^{pq})] & j \leq i \\ 0 & j > i \end{cases} \quad (58)$$

and the expression of the spatial integrals $a_{mn,1}^{pq}$ and $b_{mn,1}^{pq}$ between triangles on the dipole are given by

$$a_{mn,1}^{pq} = \int_S \int_{S'} \mathbf{f}_m^p(\mathbf{r}) \cdot \mathbf{f}_n^q(\mathbf{r}') / (4\pi R) dS' dS \quad (59)$$

$$b_{mn,1}^{pq} = \int_S \nabla \cdot \mathbf{f}_m^p(\mathbf{r}) \int_{S'} \nabla \cdot \mathbf{f}_n^q(\mathbf{r}') / (4\pi R) dS' dS \quad (60)$$

Then we consider the second testing term of the left-hand side in (56), and it becomes

$$\langle \phi_i(st), \langle \mathbf{f}_m(\mathbf{r}), L(\mathbf{e}_b(\mathbf{r}, t)) \rangle \rangle = \mu_0 s^2 \sum_{n=1}^{N_c} \sum_{p,q} \sum_{j=0}^i (0.25 e_{bn,j} + \sum_{k=0}^{j-1} (j-k) e_{bn,k})$$

$$I_{ij}(s\tau_{mn}^{pq}) a_{mn,2}^{pq} + \frac{1}{\varepsilon_0} \sum_{n=1}^{N_c} \sum_{p,q} \sum_{j=0}^i e_{bn,j} I_{ij}(s\tau_{mn}^{pq}) b_{mn,2}^{pq} \quad (61)$$

where the expression of the spatial integrals $a_{mn,2}^{pq}$ and $b_{mn,2}^{pq}$ between triangles on the dipole and triangles on the surface of the BI sphere are given by

$$a_{mn,2}^{pq} = \int_S \int_{S'} \mathbf{f}_m^p(\mathbf{r}) \cdot \mathbf{f}_n^q(\mathbf{r}') / (4\pi R) dS' dS \quad (62)$$

$$b_{mn,2}^{pq} = \int_S \nabla \cdot \mathbf{f}_m^p(\mathbf{r}) \int_{S'} \nabla \cdot \mathbf{f}_n^q(\mathbf{r}') / (4\pi R) dS' dS \quad (63)$$

Next the third term of the left-hand side of the Equation (56) is expressed as

$$\langle \phi_i(st), \langle \mathbf{f}_m(\mathbf{r}), K(\mathbf{h}_b(\mathbf{r}, t)) \rangle \rangle = s \sum_{n=1}^{N_d} \sum_{p,q} \sum_{j=0}^i \left(0.5 h_{bn,j} + \sum_{k=0}^{j-1} h_{bn,k} \right) I_{ij}(s\tau_{mn}^{pq})$$

$$d_{mn,12}^{pq} + s^2 / c_0 \sum_{n=1}^{N_d} \sum_{p,q} \sum_{j=0}^i \left(0.25 h_{bn,j} + \sum_{k=0}^{j-1} (j-k) h_{bn,k} \right) I_{ij}(s\tau_{mn}^{pq}) d_{mn,11}^{pq} \quad (64)$$

where the expression of the spatial integrals $d_{mn,11}^{pq}$ and $d_{mn,12}^{pq}$ between triangles on the dipole and triangles on the surface of the BI sphere

are given by

$$d_{mn,11}^{pq} = \int_S \int_{S'} \mathbf{f}_m^p(\mathbf{r}) \cdot \mathbf{f}_n^q(\mathbf{r}') \times \hat{R} / (4\pi R) dS' dS \quad (65)$$

$$d_{mn,12}^{pq} = \int_S \int_{S'} \mathbf{f}_m^p(\mathbf{r}) \cdot \mathbf{f}_n^q(\mathbf{r}') \times \hat{R} / (4\pi R^2) dS' dS \quad (66)$$

Similarly, we take a spatial and a temporal testing with $\mathbf{f}_m(\mathbf{r})$ ($m = 1, 2 \dots N_b$) and $\phi_i(st)$ ($i = 0, 1, 2 \dots M$) to Equations (48) and (49), and all the testing procedures can be done easily.

After applying both spatial and temporal testing procedures to Equations (47)–(49), the $(N_c + 2N_b) \times (N_c + 2N_b)$ matrix below is obtained after some mathematical manipulation,

$$\begin{bmatrix} [Z_{mn}^{e_c e_c}]_{N_c \times N_c} & [Z_{mn}^{e_c e_b}]_{N_c \times N_b} & [Z_{mn}^{e_c h_b}]_{N_c \times N_b} \\ [Z_{mn}^{e_b e_c}]_{N_b \times N_c} & [Z_{mn}^{e_b e_b}]_{N_b \times N_b} & [Z_{mn}^{e_b h_b}]_{N_b \times N_b} \\ [Z_{mn}^{h_b e_c}]_{N_b \times N_c} & [Z_{mn}^{h_b e_b}]_{N_b \times N_b} & [Z_{mn}^{h_b h_b}]_{N_b \times N_b} \end{bmatrix} \begin{bmatrix} [e_{cn,i}]_{N_c \times 1} \\ [e_{bn,i}]_{N_b \times 1} \\ [h_{bn,i}]_{N_b \times 1} \end{bmatrix} = \begin{bmatrix} [\gamma_{m,i}^{N_c \times 1}]_{N_c \times 1} \\ [\gamma_{m,i}^E]_{N_b \times 1} \\ [\gamma_{m,i}^H]_{N_b \times 1} \end{bmatrix} \quad (67)$$

To obtain the coefficients $e_{cn,j}$, $e_{bn,j}$ and $h_{bn,j}$, we need to solve the matrix recursively on the order of the degree of Laguerre function ($i = 0, 1, 2 \dots M$). Particularly at the first step when $i = 0$, only system matrix elements Z_{mn} are needed and the LU decomposition can be stored for further use. At the i th step, we only have to compute $\gamma_{m,i}$, $\gamma_{m,i}^E$ and $\gamma_{m,i}^H$ on the right side of the matrix, which are the sums of the previous solved coefficients $e_{cn,j}$, $e_{bn,j}$, and $h_{bn,j}$. The detailed expressions of these elements are given in chapter 5 of reference [24].

3. NUMERICAL RESULTS

In this section, the numerical results for a BI object loaded strip dipole in free space will be given. Triangular patches are used to mesh the strip dipole as shown in Figure 3. The delta function generator at the feeding edge is used. The inner product of the impressed field will always be zero, except for the feeding element. Therefore,

$$\langle \mathbf{F}_m(\mathbf{r}), \mathbf{E}^{\text{in}} \rangle = l_m V(t) \quad (68)$$

where l_m is the length of the feeding m -th edge, which is the strip width as shown in Figure 3. The transient Gaussian source voltage

in (68) is given by

$$V(t) = V_0 \frac{4}{\sqrt{\pi T}} e^{-\gamma^2} \tag{69}$$

where $\gamma = (4/T)(ct - ct_0)$, T is the pulse width, and ct_0 is the time delay.

The choice of factor s and maximum temporal order M is very crucial because these two parameters decide the amount of support given by the Laguerre functions in the time-domain response. For dielectric bodies problems, the initial value of these parameters are set as $M = 2BT_f + 1$, and $s = 10f_{\max}$ [22], where B and T_f are the frequency bandwidth and time duration of the excitation signal, and f_{\max} is the maximum frequency.

As the first example, the single dipole without BI object will be calculated to verify the code written in FORTRAN. As shown in Figure 1, the strip dipole is assumed to be parallel to z -axis of the coordinates. The strip dipole has a length of 1 m with 0.01 m width, and it is divided into 80 triangular patches with 79 unknowns. The Gaussian pulse of $T = 4\text{lm}$ and $ct_0 = 6\text{lm}$ is used. The unit “lm” denotes a light meter, and one light meter is the length of time taken by the electromagnetic wave to travel 1 meter in free space. The excitation is placed at the center of the strip. It is assumed that the feeding voltage amplitude V_0 is equal to 1. In the TDIE computation, we set $s = 1.0 \times 10^9$, and $M = 100$. Figure 4 displays the transient current at the center of the strip. The current is stable, and it agrees well with the results using TDIE computation based on the marching-on in time method [20]. The normalized far fields are also displayed in Figure 5 at

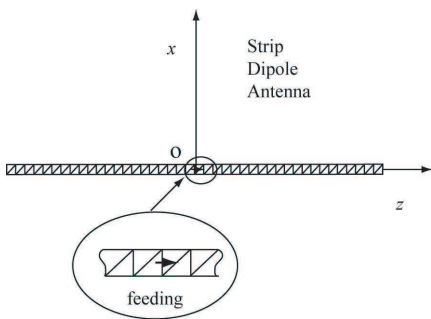


Figure 3. Triangular patching of a strip dipole.

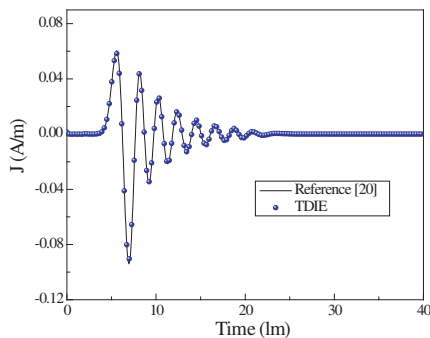


Figure 4. Transient current at the center of the strip dipole without sphere.

the direction $\theta = 90^\circ$, $\varphi = 90^\circ$, and it shows good agreement with [20]. As a special case, this exhibits somewhat the accuracy of the proposed TDIE formula for BI media loaded dipole.

As the second example, the strip dipole is placed near the bi-isotropic sphere and dielectric sphere, respectively, as shown in Figure 1. The sphere has a radius of 0.5 m, a permittivity of $\varepsilon_2 = 4.0$ with permeability of $\mu_2 = 1.0$, and it is meshed with 492 triangular patches and 738 unknowns. For the BI sphere, the Pasteur parameter and Tellegen parameter are $\kappa_r = 0.8$, and $\chi_r = 0.3$, respectively. As shown in Figure 1, the strip dipole is assumed to be parallel to z -axis of the coordinates, and the distance between the strip and the sphere center is 0.52 m. The strip dipole has a length of 1 m with 0.01 m width, and it is divided into 80 triangular patches with 79 unknowns. The Gaussian pulse remains unchanged, and the excitation is placed at the strip center. In the TDIE computation, we set $s = 5.0 \times 10^9$, and $M = 100$, which is sufficient to get a good result.

The currents of the dipole loaded with a BI sphere along the z -axis direction are shown in Figure 6. The results are compared with current distribution of single dipole and dipole loaded with dielectric sphere. It is observed that the current amplitude of BI loaded dipole is much larger than that of single dipole and DR loaded dipole. Figures 7(a) and (b) show the θ - and φ -component of the radiation far fields at the direction $\theta=90^\circ$ and $\varphi = 90^\circ$, and φ -component far fields is observed only for BI loaded dipole. The radiation patterns at the frequency 150 MHz in the XOY plane ($\theta = 90^\circ$) and YOZ plane ($\varphi = 90^\circ$) are

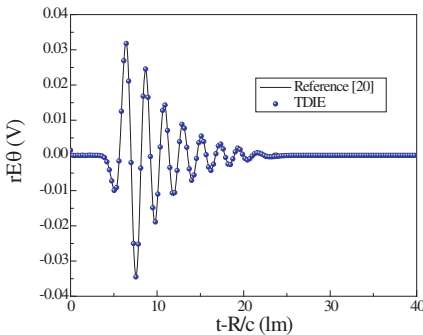


Figure 5. Radiation far-field of the single dipole in free space at $\theta = 90^\circ$, $\varphi = 90^\circ$ when the excitation signal is a Gaussian pulse.

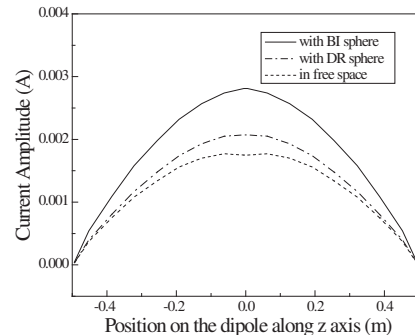


Figure 6. Current amplitude of the dipole loaded with dielectric sphere and BI sphere at the frequency of 150 MHz.

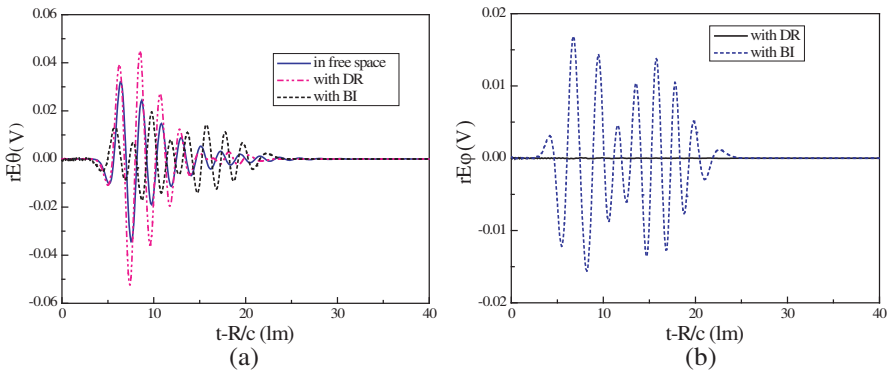


Figure 7. Transient far fields at $\theta = 90^\circ$, $\varphi = 90^\circ$ from a dipole loaded with a dielectric sphere and BI sphere. (a) θ -component. (b) φ -component.

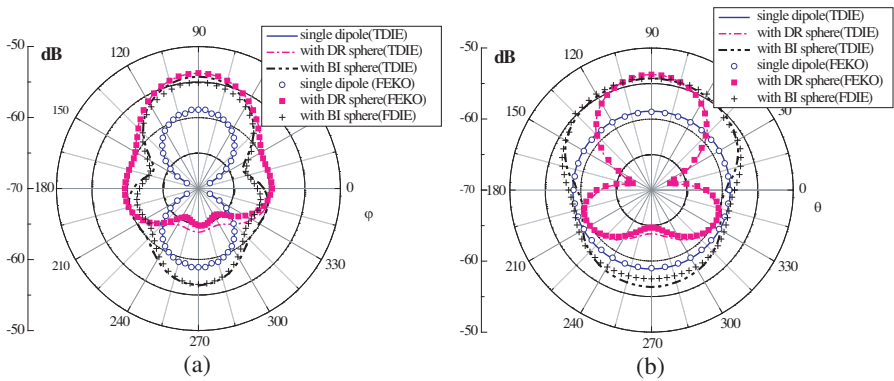


Figure 8. Radiation patterns of the dipole loaded with a BI sphere and DR sphere at the frequency of 150 MHz. (a) XOY plane. (b) YOZ plane.

demonstrated in Figures 8(a) and (b) respectively. As expected, the BI sphere strongly disturbs the symmetry of the radiation pattern. This phenomenon shows that the BI sphere has great influence on the current distribution of the dipole. The far radiation fields are displayed at a frequency of 150 MHz. The computed patterns of single dipole and DR loaded dipole are compared with the data from commercial software FEKO [29], and very good agreements are observed. The computed patterns of BI loaded dipole have been compared with frequency domain integral equation (FDIE) analysis based on the MoM

in [30], and small difference is noticed at some angles. A perfect match is not observed, and the reason is that the comparison is made between two different numerical techniques.

4. CONCLUSION

The TDIE solver based on the MOD procedure is proposed to calculate the radiation of general BI objects loaded dipole antenna. The formulas of TDIE solver for the radiation problems that are associated with the BI loaded dipole are derived. The computed results are given along with the data from previous work based on TDIE solver based on MOT method [20] and the FDIE computation based on the MoM [30]. Although only dipole loaded with BI sphere is demonstrated as example, the method is also suitable for antennas with general BI objects.

Owing to the fact that the constitutive parameters are non-dispersive, the equations abovementioned are set up for high idealized model. It is not very difficult for us to extend the proposed method for frequency dependent materials. The TDIE method based on the MOD procedure is one of the recursive convolution techniques that allow linear dispersion to be incorporated like FDTD [31, 32] formulation. The extension of the MOD based TDIE method for radiation problems of arbitrarily shaped wire antenna interacting with dispersive BI objects will be considered as the future work.

ACKNOWLEDGMENT

This work was supported by the NSFC under grant. 61001055, 10976010 and U1035002 and by the Fundamental Research Funds for the Central Universities, (SCUT), under Grant 2009ZZ0066.

REFERENCES

1. Lindell, I. V., A. H. Sihvola, S. A. Tretyakov, and A. J. Viitanen, *Electromagnetic Waves in Chiral and Bi-isotropic Media*, Artech House, Boston, MA, 1994.
2. Lindman, K. F., "Ober eine durch ein isotropes system von spiralförmigen resonatoren erzeugte rotationspolarisation der elektromagnetischen wellen," *Ann. Phys.*, Vol. 63, 621–644, 1920.
3. Tellegen, B. D. H., "The gyrator: A new electric network element," *Phillips Res. Rep.*, Vol. 3, 81, 1948.

4. Varadan, V. V., R. Ro, and V. K. Varadan, "Measurement of the electromagnetic properties of chiral composite materials in the 8–40 GHz range," *Radio Sci.*, Vol. 29, No. 1, 9–22, 1994.
5. Bahr, A. J. and K. R. Clausing, "An approximate model for artificial chiral material," *IEEE Trans. on Antennas and Propogat.*, Vol. 42, No. 12, 1592–1599, Dec. 1994.
6. Tretyakov, S. A., S. I. Maslovski, I. S. Nefedov, A. J. Viitanen, P. A. Belov, and A. Sanmartin, "Artificial Tellegen particle," *Electromagn.*, Vol. 23, No. 8, 665–680, 2003.
7. Tretyakov, S. A. and A. A. Sochava, "Proposed composite material for nonreflecting shields and antenna radomes," *Electron. Lett.*, Vol. 29, 1048–1049, Jun. 1993.
8. Engheta, N. and P. Pelet, "Reduction of surface waves in chirostrip antennas," *Electron. Lett.*, Vol. 27, 5–7, Jan. 1991.
9. Pelet, P. and N. Engheta, "The theory of chirowaveguides," *IEEE Trans. on Antennas and Propogat.*, Vol. 38, 90–98, Jan. 1990.
10. Lindell, I. V., S. A. Tretyakov, and M. I. Oksanen, "Conductor-backed Tellegen slab as twist polarizer," *Electron. Lett.*, Vol. 28, 281–282, 1992.
11. Monzon, J. C., "Radiation and scattering in homogeneous general biisotropic regions," *IEEE Trans. on Antennas and Propogat.*, Vol. 38, No. 2, 227–235, Feb. 1990.
12. Monzon, J. C., "Scattering by a biisotropic body," *IEEE Trans. on Antennas and Propogat.*, Vol. 43, No. 11, 1288–1296, Nov. 1995.
13. Kluskens, M. S. and E. H. Newman, "Scattering from a chiral cylinder of arbitrary cross section," *IEEE Trans. on Antennas and Propogat.*, Vol. 38, No. 9, 1448–1455, Sep. 1990.
14. Jaggard, D. L. and J. C. Liu, "The matrix Riccati equation for scattering from stratified chiral spheres," *IEEE Trans. on Antennas and Propogat.*, Vol. 47, No. 7, 1201–1207, Jul. 1999.
15. Wang, D. X., E. K. N. Yung, R. S. Chen, and P. Y. Lau, "Scattering characteristics of general bi-isotropic objects using surface integral equations," *Radio Sci.*, Vol. 41, No. 2, Apr. 2006.
16. Engheta, N. and M. W. Kowarz, "Antenna radiation in the presence of a chiral sphere," *J. Appl. Phys.*, Vol. 67, No. 2, 639–647, Jan. 1990.
17. Rao, S. M., *Time Domain Electromagnetic*, Academic, New York, 1999.
18. Ryne, B. P. and P. D. Smith, "Stability of time marching algorithms for the electric field integral equation," *Journal of Electromagnetic Waves and Applications*, Vol. 4, No. 12, 1181–

- 1205, 1990.
19. Davies, P. J., "On the stability of time-marching schemes for the general surface electric-field integral equation," *IEEE Trans. on Antennas and Propagat.*, Vol. 44, 1467–1473, Nov. 1996.
 20. Jung, B. H., T. K. Sarkar, Y. S. Chung, and Z. Ji, "An accurate and stable implicit solution for transient scattering and radiation from wire structures," *Microwave Opt. Technol. Lett.*, Vol. 34, No. 5, 354–359, Sep. 2002.
 21. Jung, B. H., T. K. Sarkar, Y. S. Chung, S. P. Magdalena, Z. Ji, S. Jang, and K. Kim, "Transient electromagnetic scattering from dielectric objects using the electric field integral equation with laguerre polynomials as temporal basis functions," *IEEE Trans. on Antennas and Propagat.*, Vol. 52, No. 9, 2329–2339, Sep. 2004.
 22. Jung, B. H., M. T. Yuan, T. K. Sarkar, et al., "Solving the time-domain magnetic field integral equation for dielectric bodies without the time variable through the use of entire domain Laguerre polynomials," *Electromagn.*, Vol. 24, No. 6, 385–408, Sep. 2004.
 23. Jung, B.-H., T. K. Sarkar, and Y.-S. Chung, "Solution of time domain PMCHW formulation for transient electromagnetic scattering from arbitrarily shaped 3-D dielectric objects," *Progress In Electromagnetics Research*, Vol. 45, 291–312, 2004.
 24. Wu, Z. H., "Time domain integral equations for scattering and radiation by three-dimensional homogeneous bi-isotropic objects with arbitrary shape," Ph.D. Dissertation, City University of Hong Kong, Hong Kong, Jul. 2010.
 25. Harrington, R. F., *Field Computation by Moment Methods*, New York, 1968.
 26. Rao, S. M., "Electromagnetic scattering and radiation of arbitrarily shaped surfaces by triangular patch modeling," Ph.D. Dissertation, University of Mississippi, Aug. 1980.
 27. Sihvola, A. H. and I. V. Lindell, "Bi-isotropic constitutive relations," *Microwave Opt. Technol. Lett.*, Vol. 4, No. 8, 295–297, Jul. 1991.
 28. Gradshteyn, I. S. and I. M. Ryzhik, *Table of Integrals, Series and Products*, Academic, New York, 1980.
 29. <http://www.feko.info/>.
 30. Wang, D. X., E. K. N. Yung, and R. S. Chen, "A new method for analyzing the electromagnetic characteristics of a body of complex medium," *Asia Pacific Microwave Conference*, Hong Kong, Dec. 2008.

31. Demir, V. A. Z. Elsherbeni, and E. Arvas, "FDTD formulation for dispersive chiral media using the Z transform method," *IEEE Trans. on Antennas and Propogat.*, Vol. 53, No. 10, 3374–3384, Oct. 2005.
32. Akyurtlu, A. and D. H. Werner, "BI-FDTD: A novel finite-difference time-domain formulation for modeling wave propagation in bi-isotropic media," *IEEE Trans. on Antennas and Propogat.*, Vol. 52, No. 2, 416–425, Feb. 2004.